BURNS 50 (2024) 2056–2069



Available online at www.sciencedirect.com

ScienceDirect

journal homepage: www.elsevier.com/locate/burns



The impact of subdermal adipose derived stem cell injections and early excision on systemic oxidative stress and wound healing in rats with severe scald burns



Kubilay Gürünlüoğlu [a,*], *Basri Satilmiş* [b], *Mehmet Gül* [c], *Muhammed Dündar* [d], *Nurcan Göktürk* [e], *Sami Akbulut* [b], *Ahmet Koç* [d], *Semra Gürünlüoğlu* [f], *Mehmet Aslan* [g], *Ezgi Karaaslan* [c], *Mehmet Akif Türköz* [h], *Çağla Güner Toplu* [a], *Hasan Ateş* [a], *Muhammed Mehdi Üremiş* [e], *İrem Nur Menevşe* [d], *Elif Kayhan Kuştepe* [c], *Seren Sari Ünal* [a], *Ebubekir Altundaş* [a], *Turan Yildiz* [a], *Tevfik Tolga Şahin* [b], *Sezai Yilmaz* [b], *Mehmet Demircan* [a,i]

[a] *Department of Pediatric Surgery, İnönü University, Faculty of Medicine, Malatya, Türkiye*
[b] *Department of Liver Transplantation Institute, İnönü University, Faculty of Medicine, Malatya, Türkiye*
[c] *Department of Histology and Embryology, İnönü University, Faculty of Medicine, Malatya, Türkiye*
[d] *Department of Medical Genetics, İnönü University, Faculty of Medicine, Malatya, Türkiye*
[e] *Department of Medical Biochemistry, İnönü University, Faculty of Medicine, Malatya, Türkiye*
[f] *Department of Pathology, İnönü University, Faculty of Medicine, Malatya, Türkiye*
[g] *Department of Pediatrics, Division of Pediatric Emergency Medicine, İnönü University, Faculty of Medicine, Malatya, Türkiye*
[h] *Department of Radiology, İnönü University, Faculty of Medicine, Malatya, Türkiye*
[i] *Pediatric Intensive Burn Care Unit, İnönü University, Faculty of Medicine, Malatya, Türkiye*

ARTICLE INFO

Article history:
Accepted 28 July 2024

Keywords:
Burn
Stem Cell
Early Excision
Oxidative Stress
Wound Healing

ABSTRACT

Aim: This study aims to develop an experimental treatment model effective against oxidative stress in the acute period of severe burns and to analyze the mechanisms of healing large wound defects.

Methods: Five rats, including 2 females and 3 males, were used as donors to obtain adipose-derived stem cells (ADSC) from the inguinal fat pad. The stem cells were labeled with green fluorescent protein. The study included four groups of 17 rats, each with grade 3 scalding burns on 30 % of their body surface, and a control group of 10 rats with an equal number of males and females. After early excision, 10^6 ADSC-derived stem cells were administered subdermally to the burned wound and autografted to the stem cell group (n = 17). The early excision group (n = 17) received early excision and autograft, with 2 ml of normal saline

* Correspondence to: İnönü University Faculty of Medicine Department of Pediatric Surgery, Malatya, 44315, Türkiye.
E-mail address: kgurunluoglu@hotmail.com (K. Gürünlüoğlu).

https://doi.org/10.1016/j.burns.2024.07.037
0305-4179/© 2024 Elsevier Ltd and ISBI. All rights are reserved, including those for text and data mining, AI training, and similar technologies.

injected subdermally into the burn wound edge. The PLM group (n = 17) was treated with a polylactic membrane (PLM) dressing after the burn. No treatment was given to the burn group (n = 17). Ten rats from all groups were sacrificed on the 4th day post-burn for oxidative stress evaluation. The control group (n = 10) was sacrificed on day 4. Blood and tissue samples were collected post-sacrifice. Oxidative stress and inflammation in the blood, as well as cell damage in the skin, liver, kidneys, and lungs, were investigated histopathologically and biochemically on the 4th day post-burn. On the 70th day after burn, wound healing was examined macroscopically and histopathologically.

Results: On the 4th day, oxidative stress results showed that the levels of Total Oxidative Capacity (TOC) in the blood were lowest in the stem cell (7.4 [6–8.8]), control (6.7 [5.9–7.6]), and early excision (7.5 [6.6–8.5]) groups, with no significant difference between them. The burn group (14.7 [12.5–16.9]) had the highest TOC levels. The PLM group (9.7 [8.6–10.7]) had lower TOC levels than the burn group but higher levels than the other groups.

Histopathological examination on the 4th day revealed low liver caspase-3 immunoreactivity in the stem cell and early excision groups among the burn groups. Caspase-3 immunoreactivity levels were as follows: stem cell group (20 [10–30]), early excision group (25 [15–50]), PLM group (70 [50–100]), control group (0), and burn group (80 [60–120]). Other oxidative stress and end-organ damage outcomes were consistent with these results.

All rats in the stem cell group had burn wounds that healed completely by the 70th day. Examination of the skin and its appendages from the stem cell group with an immunofluorescence microscope demonstrated green coloration, indicating incorporation of stem cells.

Conclusion: Stem cells may have the potential to form new skin and its appendages, providing better healing for large skin defects. Early excision treatment, by removing local necrotic tissues after extensive and deep burns, can prevent end-organ damage due to systemic oxidative stress and inflammation. We also believe that when these two treatments are used together, they can achieve the best results.

© 2024 Elsevier Ltd and ISBI. All rights are reserved, including those for text and data mining, AI training, and similar technologies.

1. Introduction

Burns can cause significant morbidity and mortality, affecting all age groups and genders globally [1]. Severe burns, defined as those affecting more than 20 % of the total body surface area (TBSA), can result in significant systemic effects [2]. This clinical condition is difficult to treat, with high mortality rates if early and accurate treatment is not provided[3–5]. The systemic effects of burns complicate the clinical situation, and wound healing becomes a major problem due to limited sites for obtaining autografts in patients who survive the acute period [3–5].

Early excision involves the removal of necrotic tissue (burned eschar) before spontaneous shedding or, more importantly, before the development of invasive infections [2]. Although there is no consensus on the optimal timing for early excision, it is recommended within the first few days following the burn [2]. The most successful treatment strategy for severe burns is early excision and grafting, with obtaining an adequate skin autograft being paramount for success.

Stem cells can be defined as cells that can self-renew and change into multiple cell types [6–16]. Clinically utilized stem cells are categorized according to the tissue of origin. They have the potential to differentiate into various tissue types. Adipose tissue-derived stem cells (ADSCs) are the group that is easy to obtain clinically and has good clinical results [13–16]. Stem cell therapy can be utilized to treat deep burns and skin defects [7–13]. However, the research regarding the role of stem cells in extensive and severe deep burn models is lacking. Current studies on the efficacy of stem cell therapy in burns used burn models that were not extensive and large [6–12].

In severe burn injuries, the acute period is defined as the first four days following the burn injury and is critical for the patient's prognosis. During this period, patients suffer from severe oxidative stress and inflammation, causing damage to organs such as the kidneys and lungs, and compromising wound healing [17–19]. Tumor necrosis factor-alpha (TNF-α) and interleukin-6 (IL-6) are among the factors released at the burn site, aggravating the systemic inflammatory reaction [18]. Common parameters used to evaluate oxidative stress after severe burns include total antioxidant capacity (TAC), native thiol, malondialdehyde (MDA), total oxidant capacity (TOC), and glutathione (GSH). Generally, TOC and MDA increase with oxidative stress, while native thiol, TAC, and GSH decrease due to injury-induced oxidative stress [19]. In burn injuries, the severity of inflammation and the extent of oxidative stress are correlated [20,21]. Caspase-3 expression is an important biomarker of apoptosis and tissue damage [19]. High levels of Nrf-2 (nuclear factor erythroid 2-related factor-2) play a key role in anti-oxidative mechanisms [22]. Preclinical studies have shown that end-organ damage following burn injury can be decreased by reducing oxidative stress and inflammation within the acute period following severe burns [19].

Polylactic membrane (PLM) is a modern dressing material believed to remove dead cell residues and prevent oxidative

stress due to the lactate it contains [17]. Early burn wound excision can also reduce pro-inflammatory cytokine production [23]. Hydroxyproline and transforming growth factor-beta (TGF-β) are important parameters for wound healing [19,24]. Ribosomal protein S6 (RpS6), a component of the 40 S ribosomal unit, is a marker of the wound-healing response and is associated with angiogenesis induction [25].

This study aimed to analyze the efficacy of ADSC treatment in supporting the wound healing of large defects due to severe burn injuries. Our secondary aim was to evaluate the efficacy of early excision in reducing oxidative stress and consequent end-organ damage during the acute period of severe burns.

2. Materials and methods

The experimental study commenced after receiving approval from the Local Animal Ethics Committee of İnönü University. All stages of the study were conducted in accordance with the guidelines and principles outlined in the European Union's Directive 2010/63/EU on the protection of animals used for scientific purposes.

2.1. *The donor animal procedures*

We used five 6-month-old Sprague Dawley rats weighing 250–350 g, consisting of 3 males and 2 females as donor animals. The animals were anesthetized with intramuscular injections of xylazine (10 mg/kg) and ketamine (100 mg/kg). For the anesthesia procedure, the skin on the animal's back was grasped with the left hand. After cleaning the injection site with alcohol, the needle was inserted into the muscles of the right thigh. The syringe was aspirated by withdrawing the plunger, and after it was seen that no blood was aspirated, the anesthetic agent was injected intramuscularly in a steady and fluid motion [26]. The inguinal and abdominal regions were shaved and sterilized with Povidone Iodine. A bilateral inguinal and midline skin incision was made, and the skin flaps were advanced to the flank region. The inguinal and flank fat pads were excised and immersed in chilled phosphate-buffered saline (Wisent Bioproducts, 311–010-CL) with penicillin-streptomycin (Sigma, P4083) and amphotericin B (Biological Industries, 03–028-1B).

2.2. *Isolation and cultivation of adipose derived stem cells*

The excision and isolation of adipose derived mesenchymal stem cells were performed according to the previously described technique [15,27,28]. All procedures were conducted in a biological safety cabinet (Nüve, MN120) at the Hepatology Research Laboratories of the İnönü University Liver Transplant Institute. The adipose tissues were immersed in phosphate-buffered saline in 6-well plates (SPL, 30006) for irrigation to remove remnant blood and tissue fragments. The tissues were then transferred to a 100 mm petri dish (Orange Scientific, 4450300) and minced into 1 mm^3 pieces until completely mashed. The mash was transferred to 9 ml of cell medium containing DMEM-high glucose (Sigma, D6429) and 10% v/v Penicillin-Streptomycin. One milliliter of 0.05% Type II Collagenase was added and incubated in a warm water bath (37°C) (Memmert, WNB15) for 60 min. During this period, the tubes were vortexed every 5 min for agitation and digestion. At the end of the incubation, Trypsin (Sigma, T3924) was added to the mixture and incubated for 5 min at 37°C. The tissues were agitated by vortex spinning. The digestion procedure was halted by adding Fetal Bovine Serum (FBS) (Sigma, F7524) to the DMEM-high glucose medium, and the tissues were dispersed in the solution. The tissues were centrifuged (Eppendorf, 5810 R) at 4000 rpm, + 4 °C, for 25 min. The pellet was resuspended in cell medium, the supernatant discarded, and filtered sequentially through 100 μm and 40 μm cell strainers (Labsolute 7696769, Labsolute 7696767). The cell suspension was then recentrifuged at 4 °C for 5 min at 1200 rpm. The supernatant was discarded, and the cell pellet was resuspended in DMEM-high glucose medium. Cells were counted using the Trypan Blue exclusion method (Biological Industries, 03–102-1B). Briefly, equal volumes of cells and Trypan Blue (10 μl each) were mixed. The cells were loaded onto Tukey slides and counted using an automated cell counter (Logos Luna II). The live cell count per milliliter was then calculated. The cells were cultured in a T75 cell culture flask containing DMEM with high glucose, Penicillin-Streptomycin, and Amphotericin B. They were incubated at 5% CO2 and 37 °C in an incubator (Nüve, EC160). The progression of cell culture and cell density were evaluated daily using an inverted microscope (Leica, DMi8).

Briefly, the cell culture dynamics of the ADSC is as follows; at the end of the isolation period, the viability rate of the cells is 15–20% with a total viable cell number between 500,000 to 1 × 10^6 cells/ml. It takes about 10–14 days for the SVF stem cell component to enter the log phase of cell division and once the first subculturing is performed the P2 is used for the experiments. The stem cell capabilities of the cells last for 21 days after the log phase or until P4. In addition, the cultivation process of the ADSCs selects the cells that can attach to the bottom of the cell culture flasks. Hence, stem cells attach to the bottom and other components of the SVF such as the adipose cells and endothelial cells eventually die by apoptosis and are discarded. For this reason, we did not perform an additional selection and identification step following the cultivation of the stem cells.

2.3. *Cell culture and lentivirus packaging*

In this work, 293 T (or HEK 293 T) cells were used for lentivirus production. Initially, the 293 T cells were cultured in DMEM medium supplemented with 1% penicillin and streptomycin and 10% fetal bovine serum in a 5% CO2 atmosphere at 37 °C. Before transfection, the cells were seeded at approximately 40% confluency in a 10 cm dish. Once the cells reached 70–80% confluency, the medium was replaced with the transfection complex. The transfection complex included 10 μg of pLenti-CMV-GFP-2A-Puro expression vector, 6.5 μg of pCMVdR8.74 packaging vector, 3.5 μg of pMD2. VSVG envelope vector, and 100 μl of FuGENE® HD Transfection Reagent (Promega, Madison, Wisconsin, United States) in 6.5 ml of serum-free, antibiotic-free medium. The cells were incubated in a 5% CO2 atmosphere at 37 °C for 6 h. After that, 0.65 ml of FBS was added to the medium, and the cells were

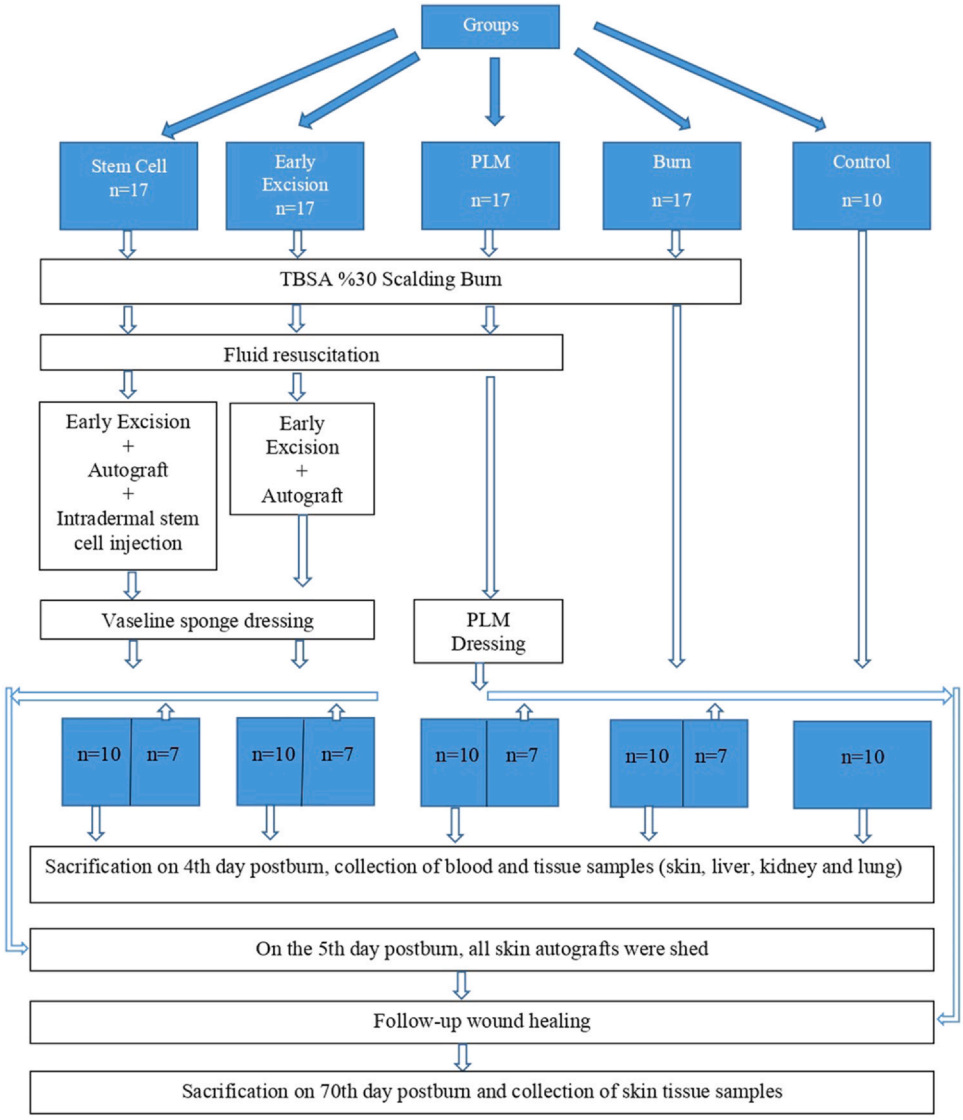


Fig. 1 – Flow chart showing the groups involved in the study and the experimental stages of the study and treatment protocols.

further incubated overnight. The next day, the transfection medium was removed, and 10 ml of complete culture medium was added to the cells. After incubating for an additional 24 h at 37 °C, the medium containing the transfected cells was centrifuged at 4 °C for 15 min at 3000 rpm to pellet any cell debris. The cleared supernatant was filtered using a low-protein binding 0.45 μm sterile filter (Millex®, Merck KGaA, Darmstadt, Germany). The filtered supernatant was stored at −80 °C as viral stock for future applications.

2.4. *Determining virus titer*

In accordance with the manufacturer's instructions, a qPCR lentivirus Titer kit (ABM Inc., Richmond, Canada) was used to determine the virus titer [29]. All samples, were run on a StepOnePlus™ Real-Time PCR System using the StepOne™ Plus v2.3 software (Applied Biosystems [AB], Foster City, CA, USA).

2.5. *Cell viability assay of ADSCs*

The cell toxicity of puromycin (Carl Roth GmbH & Co. Kg, Karlsruhe, Germany) against ADSCs was assessed using the alamarBlue assay [30]. The cells were seeded into the wells of a 96-well plate at a density of 10^4 cells per well. The plates containing the cells were then incubated in at 37 °C with a 5% CO2 atmosphere for 24 h to allow for cell attachment. Puromycin was diluted from a solution (1 mg/ml) in distilled and sterilized water to obtain target concentrations (0.0625 - 1 μg/ml). After aspirating the old medium from the wells containing the cells, 100 μl of medium containing different concentrations of puromycin was added to each well. The plates were then incubated for 24 h in a 5% CO2 atmosphere at 37 °C for the treatment. After this incubation period, cell viability percentages were determined through the alamarBlue assay [29]. The IC90 (concentration of Puromycin required for 90% inhibition) was calculated based on

the logarithmic cell viability percentages obtained from the assay.

2.6. Lentivirus transduction of ADSCs

ADSCs were seeded into a 6-well plate at a density of 2.5×10^5 cells per well 24 h prior to viral infection. The following day, the growth medium was removed from the wells and replaced with a mixture of complete medium and polybrene (Merck KGaA, Darmstadt, Germany) at a concentration of 8 μg/ml, with approximately 2.5×10^6 viral particles added per well. One well containing uninfected cells was left as the standard control. The cells were then incubated overnight with 5% CO2 37 at °C. After incubation, the culture medium was replaced with 5 ml of complete medium and the cells were incubated for another night. In order to select for stable expression of the infected cells, puromycin at a concentration of 0.25 μg/ml was used, resulting in at least 90% cell death as determined by a cell viability assay. This selection process was confirmed by flow cytometric analysis.

2.7. Flow cytometric analysis of antibiotic selection

Uninfected and selected ADSCs were subjected to flow cytometry analysis to confirm the selection of GFP-expressing cells. The cells were analyzed using the BD Accuri™ C6 Plus flow cytometer (BD Life Sciences, San Jose, CA, 95131, USA) [31]. The results were analyzed using the BD Accuri™ C6 Plus software (BD Life Sciences, San Jose, CA, 95131, USA). The software allowed for the differentiation and identification of GFP-positive cells based on their fluorescence properties.

2.8. Experimental Burn model and treatment groups

The animals used in the study were obtained from the Experimental Animal Production and Research Center at İnönü University. The experimental phase, treatment processes, and sacrifice stages of all groups in the study are illustrated in Fig. 1 as a flow diagram.

Two different power analyses were conducted, determining that a minimum of 10 rats were appropriate for assessing oxidative stress and at least 7 rats for evaluating wound healing. Thus, four groups were formed: 10 rats in the control group and 17 rats in each burn group. The rats, weighing between 250–310 g and consisting of an equal number of females and males, were randomly divided into groups [19]. One group received no treatment after burns (burn group, n = 17), while another group was treated with PLM dressing every four days (PLM group, n = 17). Wound excision was not performed on the rats in the PLM group. Burn wound dressing of the Stem cell group (n = 17) and early excision groups (n = 17) were done with a Vaseline sponge every 4 days.

We were hesitant about injecting stem cells into burnt areas with coagulation necrosis. Therefore, we developed a model consisting of debridement of the necrotic tissue caused by the burns and included 34 animals. A third experimental group was formed, and the animals underwent early excision, skin autograft, and normal saline injection into the wound (n = 17). In the fourth experimental group, we performed early excision, skin autograft, and stem cell (10^5 to 10^6 cells per animal) injection into the wound (n = 17). The skin autografts were used to prevent infection and massive fluid loss in the early period after establishing the burn model. All skin grafts sloughed off within 3–5 days following the establishment of burn injury and application of the dermal graft. Finally, there was a sham (control) group of 10 rats where no procedure was performed. The animals were sacrificed, and tissue and serum samples were obtained to determine the normal structure and serum levels of laboratory parameters.

Anesthesia and analgesia were administered 20 min before the procedure. For anesthesia, an insulin injector was used to administer 10 mg/kg of xylazine (Sanalazin 100; Santavet, Istanbul, Türkiye) and 100 mg/kg of ketamine (Keta-Control; Doğa Pharmaceuticals, Istanbul, Türkiye) intramuscularly into the right thigh muscle [26]. As an analgesic, 100 mg/kg of paracetamol (Partemol; VEM Pharmaceuticals, Ankara, Türkiye) was administered intraperitoneally [19].

As in the previous study, the area of a 30% TBSA was calculated based on the weight of the rats before the burn, using Meeh's constant [19,32,33]. The calculated ridge area was then shaved. Next, a burn model was created by immersing the ridge area in water at 95 °C for 15 s [19]. Finally, the burned skin of the rats in the early excision group and the stem cell group was immediately excised after the burn procedure. After excision of the burnt skin, an equal amount of 2 ml solution containing 10^6 stem cells was injected subdermally into the intact skin, 1 cm proximal from the wound edge and 1 cm apart, for each rat in the stem cell group. In the early excision group, 2 ml of normal saline was injected subdermally at 1 cm proximal to the wound edge and 1 cm apart. An ellipsoid-shaped skin graft with a short radius of 1.5 cm and a long radius of 2 cm was removed from the abdominal skin of the rats in the early excision group and stem cell groups, as a full layer. Grafts were added to female and male rats at the wound edge with an open wound of 1 cm in all directions so that the wound would not be closed. Our aim was to apply insufficient grafts. The defect was then closed by continuous suturing with a 4/0 absorbable suture. The removed full-thickness skin graft was placed in the middle of the excised wound area by suturing with 4/0 absorbable sutures.

Fluid resuscitation of all rats with burn injuries was performed by administering 4 ml x weight (kg) x % TBSA burn of Ringer's lactate intraperitoneally, following Parkland's formula [19]. The wound surface of the stem cell group and the early excision group was dressed with a Vaseline sponge, and the PLM group was dressed with a wound dressing containing PLM every four days. All rats were weighed at the start of the study and just before they were sacrificed. This data was recorded. All rats had free access to food and water and were fed the same rat food. Daily activity monitoring of all rats was carried out regularly.

2.9. Isolation of RNA from tissues

To isolate RNA samples, 30 mg of each tissue sample (lung, liver, and kidney) was measured and homogenized using a

bead beater (Mini-Beadbeater-24, BioSpec Products Inc., Bartlesville, USA). Total RNA from homogenized tissue samples of all experimental groups was extracted using the RNeasy® Mini Kit (Qiagen, Hilden, Germany) following the manufacturer's instructions. The extracted RNA was then quantified using a spectrophotometer (Denovix DS-11 FX+, Denovix Inc., Wilmington, USA) and stored at −80 °C until further analysis.

2.10. RT-qPCR analysis

RNA samples were reverse-transcribed using the "ProtoScript® First Strand cDNA Synthesis Kit" from New England Biolabs, USA. The BlasTaq™ 2X qPCR MasterMix from Applied Biological Materials Inc. (abm) in Richmond, Canada was used for the reaction. Each sample was analyzed in triplicate. The primer sequences for the Caspase-3 gene were as follows: forward: 5′-CCTGTGATTGGAGAGAAGA TGG-3′ and reverse: 5′-GGAGTCCAGTGAACTTTCTTGA-3′. The primer sequences for the Actb (actin beta, endogenous control) gene were as follows: forward: 5′-GGAGATTACTGCCCT GGCTC-3′ and reverse: 5′-GACTCATCGTACTCCTGCTT-3′. The qPCR conditions were as follows: 95 °C for 10 min, followed by 40 cycles of 95 °C for 15 s and 60 °C for 30 s, concluding with a melting curve analysis. Using CT values, the relative expression level of the Caspase-3 gene compared to the Actb gene was analyzed for each sample using the Livak method [34].

2.11. Collection of tissue and blood samples from rats sacrifice

Seven rats from each group were sacrificed on the 70th day of the study to evaluate wound healing, and ten rats from each group were sacrificed at the end of the fourth day to examine the effects of oxidative stress on the groups. The sacrifice procedure was performed by anesthetizing the rats with xylazine and ketamine at the doses used for the burn model, followed by aspirating the maximum blood volume (4–10 ml) from the precordium using a syringe. Tissue samples were then collected.

2.12. Wound healing

To evaluate macroscopic wound healing, the burn wound area of each rat was measured from seven rats in four groups where the burn model was applied on the first day of the study. Since the burned area created resembled an ellipse, the wound area was calculated using the formula for the area of an ellipse (Supplementary Figure 1).

The area formula for an ellipse is calculated by multiplying the short radius, long radius, and the constant of PI ($\pi = 3.14$). The **area of the first burn wound**, calculated with the data from the beginning, was recorded in square millimeters. To monitor wound healing, wound site photographs of 7 rats from each group (except for control) were taken at a distance of 20 cm every 3–4 days. This process continued until all the rats in one of the groups had their wounds closed. The study was terminated on the 70th day when the burn wounds of all rats in one of the groups had closed. The wounds of only the rats in one group (stem cell group) were completely healed. On the 70th day post-burn, the final wound area of the rats in all groups was measured, and the macroscopic healing area was recorded in square millimeters. The **final macroscopic wound areas** were then statistically analyzed between the groups and the difference among groups was investigated. After the rats were sacrificed, a 1 cm wide and 3 cm long section in the middle of the burn wound was excised at full thickness and a skin tissue sample was created for histopathological examination.

2.13. Biochemical analyses

At the end of the study, blood and skin samples were taken from anesthetized rats. The blood samples were centrifuged at 4000 rpm for 10 min at +4 °C. The serum samples were aliquoted and stored at −80 °C until analyses. BUN, Creatinine, LDH, AST, ALT, Total Antioxidant Capacity (TAC), Total Oxidant Capacity (TOC), Native Thiol, TNF-α, and IL-6 analyses were performed in the serum samples. The skin samples were stored at −80 °C until the Nrf2, TGF-β1, MDA, GSH, and hydroxyproline analyses.

The levels of serum BUN, Creatinine, LDH, AST, and ALT were measured using commercial kits (Beckman Coulter, Inc. USA) with a clinical chemistry analyzer (Beckman Coulter AU5800).

The levels of serum TNF-α and IL-6 were measured using commercial ELISA kits according to the instructions provided by the manufacturer (Bostonchem, Boston, USA). The levels of serum TAC, TOC, and Native Thiol were measured using commercial kits according to the protocol provided by the manufacturer (Rel Assay Diagnostics, Gaziantep, Turkey).

Half of the skin samples were frozen in liquid nitrogen on the day of the experiments. The frozen samples were crushed into small pieces using a weight on a hard surface and were homogenized using a mechanical homogenizer after adding phosphate-buffered saline. The skin homogenates were used to determine the levels of TGF-β1, Nrf-2, MDA, and GSH. The levels of TGF-β1 and Nrf-2 using commercial ELISA kits according to directives provided by the manufacturer (Elabscience Biotechnology, USA). MDA analysis was performed according to Ohkawa's spectrophotometric method [19]. GSH analysis was performed according to Ellman's spectrophotometric method [19].

The other half of the skin samples were used to measure the level of hydroxyproline. Hydroxyproline analysis was performed according to the Reddy's spectrophotometric method [19].

2.14. Histopathological evaluation

The liver, lungs, and kidneys that were excised on the 4th day following the burn injury and the skin samples taken at the end of the study were used for the histopathological analyses. The histopathological method and scoring systems used were performed as described in our previous study [19]. The tissues were fixed in 10% formalin for 48 h. All tissue samples were then dehydrated through a series of ethanol solutions (50%, 70%, 80%, 96%, and absolute). Sections of 6 µm thickness were cut from the paraffin blocks using a microtome and placed on microscope slides. All sections

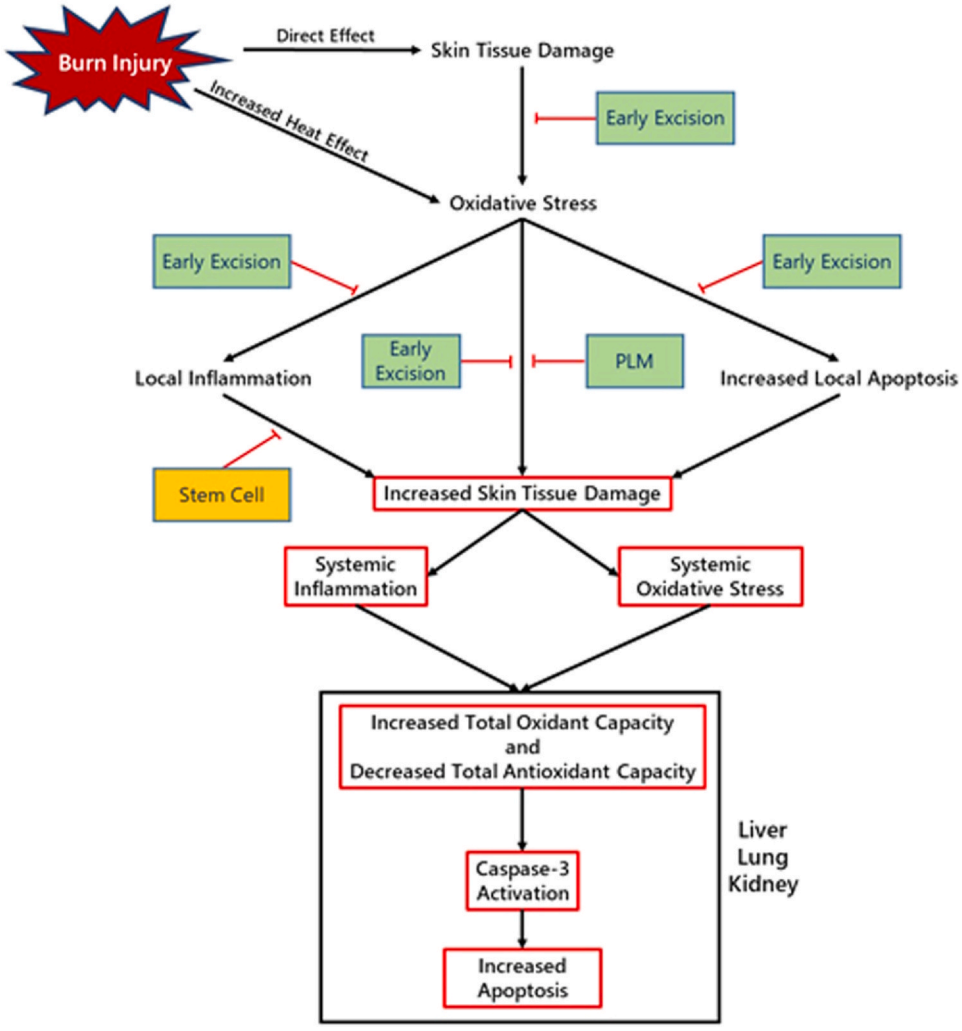


Fig. 2 – - Diagram summarizing the chain of events up to the 4th day following a burn leading to organ damage. Also, the mechanisms of action of stem cell, early excision and polylactic membrane in this chain of events are shown.

were stained with hematoxylin-eosin (H-E). In addition, the immunoreactivity of anti-RpS6 (Ribosomal Protein S6 monoclonal antibody sc-74459 Santa Cruz Biotechnology, Dallas, TX, USA; dilution ratio: 1:300) on skin sections and the immunoreactivity of anti-caspase-3 (Caspase-3 monoclonal antibody sc-56053; Santa Cruz Biotechnology, Dallas, TX, USA; dilution ratio: 1:300) on lung, liver, and kidney sections were determined by the standard immunohistochemical method.

The stained sections were examined with a light microscope (Nikon Eclipse Ni-U, Nikon Corporation, Tokyo, Japan) and its associated camera, and evaluated using the image analysis program (Nikon NIS-Elements Documentation 5.02) from the same camera system.

In skin sections, inflammatory cells, ulceration/necrosis, and edema were scored (absent = 0, mild = 1, moderate = 2, severe = 3) with a maximum total damage score of 9. Additionally, the epithelialization/keratinization of the epidermal layer at the burn site was assessed and scored (0 - no epithelialization, 1 - partial epithelialization, 2 - continuous epithelialization, 3 - continuous epithelialization and keratinization) [19].

In lung sections, inflammatory cell infiltration, thickening of the interalveolar septum, and vascular and capillary congestion were scored on a scale of 0 (absent) to 3 (severe) for each category, with a maximum total damage score of 9 [19].

Histopathological changes in liver sections, such as inflammatory cell infiltration, hepatocyte necrosis, and hydropic damage to hepatocytes, were scored on a scale of 0 to 3 (with 0 indicating no damage, 1 indicating mild damage, 2 indicating moderate damage, and 3 representing severe damage). In this assessment, the maximum damage score was considered to be 9 [19].

Kidney damage was assessed by grading the accumulation of material in the tubule lumen, as well as any tubular and glomerular damage. The grading for tubular injury was as follows: grade 0 absent, grade 1: < 25% of tubules injured, grade 2: 25–50% of tubules injured, and grade 3: < 50% of tubules injured. Glomerular damage was evaluated based on the following scale: grade 0 for absence, grade 1 for < 25% of glomeruli affected, grade 2 for 25–50% of glomeruli affected, and grade 3 for < 50% of glomeruli affected. The maximum possible damage score was 9 [19].



Fig. 3 – - Image of wound healing between 0 and 70 days post-burn of a rat from the stem cell group.

A semi-quantitative H-score system (H-score = staining intensity x percentage of stained cells) was used to determine the immunoreactivity of caspase-3 in lung, liver, and kidney sections, and the immunoreactivity of RPS6 in skin sections. Staining intensity was rated on a scale of 0–3 (no staining = 0, weak staining = 1, moderate intensity staining = 2, and strong intense staining = 3), and the percentage of stained cells. The H-scores ranged from 0 to 300.0 [19].

2.15. *Immunofluorescence microscopic evaluation*

Frozen sections were prepared from 0.5 × 0.5 cm skin samples taken at the end of the study. The skin samples were prepared, sectioned, and examined under the immunofluorescence microscope (Nikon Eclipse Ni-U) using a GFP/FITC filter (excitation 395–475 nm, emission 510 nm).

3. Statistical analysis

The normal distribution of the data was checked by Shapiro-Wilk test. Quantitative data showing normal distribution were summarized with mean ± standard deviation, while quantitative data not showing normal distribution were summarized with median (95% confidence interval). In statistical analyses, dependent samples t-test was used for before and after tests, and one-way analysis of variance and Kruskal-Wallis tests were used in independent group analyses considering normal distribution. In the analyses, $p < 0.05$ was considered significant. Analyses were performed using IBM SPSS 25.0 and TURCOSA statistical software (Turcosa Analitik Ltd. Co., Kayseri/Türkiye). Fig. 2.

4. Results

We presented our results in two parts. The first part includes our results regarding oxidative stress. The second process includes our results regarding wound healing.

Skin autografts in all rats in the early excision group and stem cell groups were completely shed off within 5 days after the surgical procedure. Thus, the wounds of these rats became open wounds and were dressed in a Vaseline sponge. We think that autografts fall out due to the absence of solid subcutaneous ground, where they could receive blood support, because the burn is deep.

There were no significant changes in the weight of the animals at the beginning and at the end of the study. Furthermore, there are no significant differences among the study groups. The results regarding the weight changes of the experimental groups are summarized in Supplementary Table 1.

4.1. *Oxidative stress on the fourth day after the burn, as well as the consequences of damage to the end-organs*

4.1.1. *Results of Biochemical Analyses*

The effects of burn-related oxidative stress and inflammation up to 4. day after the burn are shown in Fig. 3.

The skin oxidative stress parameters of the study groups at the 4th day are shown in Supplementary Table 2. The results of oxidative stress and inflammation parameters at the 4th day for each group are shown in Table 1.

The tissue levels of Nrf-2 in burned skin were lowest in the burn and PLM groups (Supplementary Table 2). The burn group had significantly higher MDA levels, while the control group, stem cell group, and early excision group had significantly lower MDA levels (Supplementary Table 2). The group with the highest MDA level in the burned skin was found the Burn group. The PLM group was found to be having the second highest MDA level in the burned skin. (Supplementary Table 2). The burned skin in the burn group had the lowest GSH levels (Supplementary Table 2). GSH levels were the highest in the stem cell and early excision groups. There was no significant difference between the control and PLM groups in GSH levels (Supplementary Table 2). The tissue level of TGF-β1 was found to be highest in the stem cell group (Supplementary Table 2). In the control group, TGF-β1 levels were lower than the stem cell group but higher than the other groups (Supplementary Table 2). TGF-β1 levels were low in the burn, PLM, and early excision groups; with no significant difference among these groups (Supplementary Table 2). Highest levels of hydroxyproline were found in the stem cell and burn groups (Supplementary Table 2). The stem cell group showed higher levels of hydroxyproline compared to the other groups. Hydroxyproline levels were lowest in the control, PLM, and early excision groups. No significant difference was observed among these three groups (Supplementary Table 2).

The results of oxidative stress and inflammation parameters of the study groups are summarized in Table 1. In the statistical analysis of TNF-α and IL-6 levels, there was no significant difference in the stem cell, control and early

Table 1 – Summary of the serum oxidative stress, markers of end-organ damage, and inflammation.

Variable*	Groups** Stem cell (n=10)	Early Excision (n=10)	PLM (n=10)	Control (n=10)	Burn (n=10)	p
IL-6(pg/ml)	19.9[a] (16.8-22.9)	17.3[a] (14.8-19.7)	53.9[b] (48.9-58.8)	10.7[a] (8.8-12.5)	143.7[c] (119.9-167.4)	**<0.001**
TNFα(pg/ml)	16.9[a] (13.2-20.6)	17.7[a] (14.5-20.8)	57.2[b] (52.1-62.2)	14.3[a] (11.7-16.9)	109.1[c] (95.2-122.9)	**<0.001**
TOC (μmol H2O2 Equiv/L)	7.4[a] (6-8.8)	7.5[a] (6.6-8.5)	9.7[b] (8.6-10.7)	6.7[a] (5.9-7.6)	14.7[c] (12.5-16.9)	**<0.001**
TAC(μmol•Trolox•equiv/L)	0.69[a] (0.60-0.78)	0.65[a] (0.58-0.72)	0.54[b] (0.47-0.60)	0.70[a] (0.61-0.79)	0.27[c] (0.21-0.33)	**<0.001**
Native Thiol(umol/L)	101.2[a] (92.8-109.6)	97.9[a] (85.6-110.2)	67.3[b] (57.4-77.2)	116.5[a] (111.3-121.6)	36.7[c] (31.7-41.7)	**<0.001**
BUN (mg/dL)	20.2 (19.6-22.8)	19.8(18.5-20)	19.4(18.6-20.5)	19.1(18.2-21.2)	20.7(19.6-22.2)	0.5
Creatinine (mg/dL)	0.35(0.3-0.4)	0.35(0.3-0.4)	0.4(0.4-0.4)	0.3(0.3-0.4)	0.4(0.4-0.5)	0.6
LDH (U/L)	142[a] (124-168)	154.5[a] (141-169)	168[a] (150-187)	158[a] (153-171)	296[b] (241.9-353)	**<0.001**
ALT (U/L)	53.5[a] (45-68)	53.5[a] (44-64)	50[a] (41-62)	56[a] (48-62)	138.5[b] (114-164)	**<0.001**
AST (U/L)	111[ab] (98-132)	101.5[ac] (98-112)	118[b] (104-132)	95.5[c] (84-118)	665[d] (519-836)	**<0.001**

Abbreviations: IL-6: Interleukin-6, TNF-α: Tumor necrosis factor-alpha, PLM: Polylactic membrane, TOC: Total oxidant capacity, TAC: Total antioxidant capacity, AST: Aspartate aminotransferase, ALT: alanine aminotransferase, BUN: Blood urea nitrogen, LDH: Lactate dehydrogenase.

* Variables are summarized as 'median (95% confidence interval)

** The difference between the groups with different superscript letters are statistically significant. There is no statistically significant difference between groups with identical superscript letters.

excision groups and was found to be low. (Table 1). The burn group had the highest levels of TNF-α and IL-6 in the blood (Table 1). The PLM group had lower levels of TNF-α and IL-6 than the burn group, but higher levels than the other groups (Table 1). TOC levels were lowest in the stem cell, control, and early excision groups. There was no significant difference between these groups. The burn group had the highest serum levels of TOC. The PLM group had lower levels of TOC than the burn group, but higher levels than the other groups (Table 1). TAC levels were higher in the stem cell, control, and early excision groups, with no significant difference among them (Table 1). The burn group had the lowest serum TAC levels. The PLM group had higher TAC levels than the burn group, but lower than the other groups (Table 1). Serum Native Thiol levels were higher in the stem cell, control, and early excision groups, with no significant difference among them (Table 1). The burn group had the lowest serum Native Thiol levels (Table 1). The PLM group had higher Native Thiol levels than the burn group, but lower levels than the other groups. There was no significant difference in BUN and creatinine levels among the groups (Table 1). The burn group had a significantly higher serum ALT and AST levels than the other groups. The stem cell-treated group had significantly lower serum AST levels than the other groups (Table 1).

4.1.2. *End-organ histopathological evaluation results at the 4th day postburn*

The relative Caspase-3 expression was highest in lungs, kidneys, and liver tissues in the burn group. In the PLM group, relative Caspase-3 expression in lungs, kidneys, and liver tissues was significantly lower than the burn group, but higher than the other three groups. The relative Caspase-3 expression was lowest in the lungs, kidneys, and liver tissues of the stem cell, early excision, and the control groups, found to be the. There was no difference in relative Caspase-3 expression between these three groups. The results of the relative Caspase-3 expressions are summarized in Supplementary Table 3.

4.1.2.1. *Lungs*.

The results of the histopathological analyses are summarized in Table 2. In the H&E-stained lung sections of the control group, vascular structures, lumens of bronchi, and bronchioles were observed in an open and normal histological structure. Alveolar sacs and interalveolar septa in the lung parenchyma were evaluated as normal histological structure (Table 2).

Vascular congestion, intense inflammatory cell infiltration in perivascular areas, and perivascular edema were observed in the lung sections of the burn group. In the lung parenchyma, areas with thickening of the interalveolar septa, closure of the alveolar sacs, and intense inflammatory cell infiltration were found. Capillary congestion and hemorrhage were also noted in these areas (Table 2).

The vascular structures, bronchi, and bronchioles were evaluated in their normal histological structure in lung sections belonging to the stem cell and early excision groups. There was minimal inflammatory cell infiltration present in some perivascular areas. Additionally, there was minimal thickening of the interalveolar septa in some areas of the lung parenchyma (Table 2).

Although there were regressed findings of histopathological damage in the lung sections of the PLM group compared to those in the burn group, there were still observed signs of inflammatory cell infiltration, perivascular edema, and thickening of the interalveolar septa (Table 2).

Analyses of the immunohistochemical evaluation of the Caspase 3 showed that H-score was control (0), Burn (100(80–120)), Stem cell (20(10–40)), Early excision (30(20–50)) and PLM (100(60–120) (Table 2).

4.1.2.2. *Liver*.

The histopathologic analyses of the liver are summarized in Table 2 and Supplementary Figures 2 and 3. The hepatocyte cords, sinusoids, central vein, and portal areas in the liver parenchyma were normal in the control group.

The hepatocyte cords, sinusoids, central vein, and portal areas in the liver parenchyma were found to exhibit normal

Table 2 – Summary of the histopathological examination and Caspase-3 antigen in the Lungs, Liver, and Kidneys tissues of the study groups 4 days after the burn injury.

	Groups*					
The end organ damage on the 4th day postburn	Stem cell (n=10)	Early excision (n=10)	PLM (n=10)	Control (n=10)	Burn (n=10)	*p*
Lungs						
Inflammatory cell infiltration	1(1-2)[a]	1.5(1-2)[a]	2(1-2)[b]	0(0-0)[c]	2(2-3)[d]	**< 0.001**
Thickening of interalveolar septum	1(1-2)[a]	1(1-2)[a]	1.5(1-2)[b]	0(0-0)[c]	2(1-2)[d]	**< 0.001**
Vascular and capillary congestion	0(0-1)[a]	1(1-2)[b]	1(1-2)[c]	0(0-0)[d]	2(1-2)[e]	**< 0.001**
Total damage score	3(2-4)[a]	3(2-5)[a]	5(4-6)[b]	0(0-0)[c]	6(5-6)[d]	**< 0.001**
Caspase 3 immunoreactivity	20(10-40)[a]	30(20-50)[a]	100(60-120)[b]	0(0-0)[c]	100(80-120)[d]	**< 0.001**
Liver						
Inflammatory cell infiltration	0(0-1)[a]	1(0-2)[b]	1.5(1-2)[c]	0(0-0)[d]	1.5(1-2)[c]	**< 0.001**
Hepatocyte necrosis	0(0-0)[a]	1(0-1)[b]	1(0-1)[b]	0(0-0)[a]	1(1-2)[c]	**< 0.001**
Hydropic damage to hepatocytes	0.5(0-1)[a]	1(0-2)[a]	1.5(1-2)[b]	0(0-0)[c]	2(1-3)[d]	**< 0.001**
Total damage score	0.5(0-2)[a]	1(0-3)[a]	4(2-5)[b]	0(0-0)[c]	4.5(3-6)[d]	**< 0.001**
Caspase 3 immunoreactivity	20(10-30)[a]	25(15-50)[a]	70(50-100)[b]	0(0-0)[c]	80(60-120)[d]	**< 0.001**
Kidneys						
Tubular damage.	1(1-1)[a]	1(1-2)[a]	2(1-2)[b]	0(0-0)[c]	2(2-3)[d]	**< 0.001**
Accumulation of material in the tubule lumen.	0(0-1)[a]	1.5(1-2)[b]	2(1-2)[b]	0(0-0)[c]	2(1-3)[d]	**< 0.001**
Glomerular damage.	0(0-1)[a]	0.5(0-1)[a]	1(0-1)[b]	0(0-0)[c]	1(0-1)[b]	**< 0.001**
Total damage score.	3(2-4)[a]	3(2-4)[a]	5(4-6)[b]	0(0-0)[c]	5(3-6)[d]	**< 0.001**
Caspase 3 immunoreactivity.	25(10-40)[a]	30(10-60)[a]	60(40-80)[b]	0(0-0)[c]	80(60-100)[d]	**< 0.001**

* The difference between the groups with different superscript letters are statistically significant. There is no statistically significant difference between groups with identical superscript letters.

histology in H&E-stained liver sections of the control group (Supplementary Figure 2) (Table 2).

Histopathological damage findings were significantly improved in the liver sections of the stem cell and early excision groups compared to those in the burn group. In these groups, minimal inflammatory cell infiltration and hydropic changes in the cytoplasm of some hepatocytes were detected (Supplementary Figure 2a-b) (Table 2).

Histopathological damage findings regressed in the liver sections of the PLM group compared to those in the burn group. Inflammatory cell infiltration in the liver parenchyma, as well as hydropic changes in the cytoplasm of hepatocytes and focal necrosis areas, were observed in the liver parenchyma (Supplementary Figure 2c) (Table 2).

In the liver sections from the burn group, areas of necrosis were seen in the liver parenchyma. Inflammatory cell infiltration was noted in parenchymal necrosis sites, as well as in portal and periportal regions. Marked hydropic changes were commonly observed in the cytoplasm of hepatocytes **(**Supplementary Figure 2e) (Table 2).

The immunohistochemical analyses for the anti-caspase-3 staining showed that Caspase-3 antigen distribution was prominent, particularly in pericentral hepatocytes (Supplementary Figure 3**)**. The H-score for caspase-3 immunoreactivity was determined as follows: stem cell group (20 (10–30)), early excision group (25 (15–50)), and PLM group (70 (50–100), control group (0), burn group (80 (60–120)), (Supplementary Figure 3a-e) (Table 2).

4.1.2.3. *Kidneys*. The results of the histopathologic analyses of the renal tissues are summarized in Table 2. The normal histological structure of the glomeruli, proximal and distal tubules, and interstitial tissue were evaluated in the H&E-stained kidney sections of the control group (Table 2).

In the burn group, cell lysis was observed in some glomeruli and narrowing and closure of the Bowman space were noted. Damage to the proximal and distal tubule epithelium and total tubular degeneration were also detected. Furthermore, the lumen of some tubules showed an accumulation of eosinophilic hyaline material (Table 2).

Although there was a significant improvement in the histopathological damage findings for the kidney sections of the stem cell and early excision groups compared to the burn group, there was minimal epithelial damage in the proximal and distal tubules. There was only a slight accumulation of eosinophilic hyaline material in the lumens of some tubules in the kidney sections of the stem cell and early excision group (Table 2).

The findings of histopathologic damage of the renal tissues of the PLM group showed regression compared to those in the burn group but epithelial damage was still observed in the renal tubules and there was an accumulation of eosinophilic hyaline material in the lumen of the tubules (Table 2).

The immunohistochemical analyses of the caspase-3 staining showed that the H-score for caspase-3 immunoreactivity was as follows: stem cell group (25 (10–40)), early excision group (30 (10–60)), PLM group (60 (40–80)), control group (0), Burn group (80 (60–100)) (Table 2).

4.2. *Burn wound healing results on the seventieth day*

4.2.1. *Macroscopic wound healing on the seventieth day*

When comparing the burn wound area in all burn groups at the beginning of the study, it was found that there were no significant differences in the size of the burn areas between the groups (Table 3). Fig. 3 **to** Supplementary Figures 4–6 summarize the wound healing process for the stem cell, early excision group, PLM, and burn groups.

We considered complete closure of the burn wound as a parameter, a success criterion in wound healing. On the

Table 3 – The changes in the wound surface area at the beginning and the end of the study (0th- 70th day postburn).

	Groups				
Burn Wound area (mm^2)	Stem cell (n=7)	Early excision (n=7)*	PLM (n=7)	Burn (n=7)*	p**
Initial burn wound area (mm^2)	4819.5(4603.3-5035.6)	4825.7(4575-5076.5)	4865.2(4649.1-5081.3)	4908.6(4659.9-5157.4)	**0.904**
Final burn wound area (mm^2)	0^a	2261.6^b(2128-2395.2)	1486.7^c(1358-1615.3)	2479.4^d(2328.2-2630.7)	**< 0.001**

* Early excision – Burn (b-d) (p=**0.041**).
** The difference between the groups with different superscript letters are statistically significant. There is no statistically significant difference between groups with identical superscript letters.

seventieth day after the burn, the stem cell group had the most successful macroscopic wound healing among all the postburn groups (Table 3). Out of the groups of the burn model was created, only the stem cell group had a completely closed burn wound. Therefore, the stem cell group was the only successful group. It was also found that the other three groups failed in wound healing in wound closure (Table 3).

Although PLM, burn and early excision groups were considered unsuccessful because the burn wound did not close, we measured the wound area among them. At the end of seventy days, the wound area was smaller in the PLM group compared to the early excision and burn groups (Table 3). The wound area of the early excision group was significantly smaller than the burn group (Table 3).

4.2.2. *Histopathological examination in skin tissues on the seventieth day*

The histopathologic analyses of the skin tissues obtained on the 70th day and the RpS6 immunoreactivity examination are presented in Supplementary Table 4. In the H&E-stained skin sections of the control group, normal morphology was observed (Supplementary Table 4).

Epithelialization was generally not observed on the surface in the sections belonging to the burn group. Ulcerated or necrotic tissue residues were present in some areas on the surface. It was determined that the collagen structure of the connective tissue was impaired in the superficial portions of the dermis layer, and the cell density of the connective tissue decreased. Diffuse edema was present in both the dermis and hypodermis layers. In certain sections, hemorrhage was observed in the hypodermis layer, particularly in the perivascular areas (Supplementary Table 4).

Histopathological damage findings improved significantly in the stem cell group. In most sections, the epidermis was observed as keratinized and non-keratinized multi-layered squamous epithelial tissue containing 1–3 rows of keratinocyte layers. Although the dermis and hypodermis layers mostly had a normal histological structure and cellular content, minimal inflammatory cell infiltration and edema were present in some areas (Supplementary Table 4).

In the early excision and PLM groups, areas of the epidermis containing 1–2 sequential keratinocytes on the surface were observed, generally showing nonkeratinized epithelization. Additionally, there was regression in histopathological damage findings in the early excision group and PLM groups compared to the burn group. However, there were still minimal inflammatory cell infiltration, edema, and ulcerated/necrotic tissue in some areas. The total skin damage score in the PLM group was not different from the early excision group. However, epithelialization and RpS6 immunoreactivity in the PLM group were found to be lower than in the stem cell group, and significantly higher than in the early excision and burn group (Supplementary Table 4).

In the sections where immunohistochemical anti-RpS6 staining was applied, the highest immunoreactivity H-score was found in the stem cell group (Supplementary Table 4).

The RpS6 immunoreactivity of the groups was found as follows; 240 (200–300) in the stem cell group, 120 (100–160) in the early excision group, 15 (10–20), 170 (140) in the PLM group, in the control group and 100 (80–120) in the burn group (Supplementary Figure 7a-e) (Supplementary Table 4).

4.2.3. *Immunofluorescence microscopic evaluation in skin tissue on the seventieth day*

The cells labeled with green fluorescent protein were present in all layers of the skin in the stem cell group (Supplementary Figure 8).

5. Discussion

Our main goal in conducting this study was to create a model in which the burn surface area was extensive and the autograft applicability had been inadequate application of skin autografts in severe full-thickness burns because this was the most important problem we faced clinically. Skin autograft application is already the gold standard for successfully treating patients with full-thickness extensive burns, provided that there are sufficient grafts available. Therefore, the graft was applied in such a way that it did not completely close the wound and was not expanded. However, intradermal injection of stem cells may be a new treatment method for patients with deep and wide burns, for whom this method is impossible to perform by applying intradermal stem cell injections together with a skin autograft that partially closes the wound (although the grafts have fallen out), we have created the model we were aiming for. The results of the present study are striking. We have observed complete wound closure in ADSC treated group. Stem cells can be an effective novel therapy for severe and deep burn injury. Oxidative stress that occurs after burns can have negative effects on the healing of the burn wound and may cause damage to end organs such as the lungs, kidneys, and liver [35]. Especially in severe and deep burns, excision of the burned skin area is performed which results in reduction of the detrimental effects of the burn injury. The impact of oxidative stress is minimal in both the stem cell and early excision groups, as

these two groups underwent burnt skin removal procedures. The unfavorable effects of oxidative stress on the stem cell group are similar to those of the early excision group. We believe that the positive results observed in the stem cell group are due to both the early excision process that eliminates the damaged tissue and the immunomodulation effect of stem cells to reduce inflammation. Neither PLM dressing, which is a modern dressing method, nor early excision applications, have not been successful in closing large burn wound defects. Based on our study, we suggest that early excision of the burn wound with stem cell injection at the wound edges is the most effective treatment method for severe burns with large skin defects. At the end of the study, only the stem cell group showed complete healing of the burn wound. Based on these findings, it can be concluded that the stem cell group outperformed all other groups in macroscopic wound healing. We believe that stem cells support wound healing through their regenerative capacity. Microscopic examination of the healing skin in this group at the end of the study revealed the presence of green fluorescent cells in all layers of the skin. One of the most important results of the study is the immunoreactivity of RpS6 in the skin, which is one of the parameters used to evaluate wound healing. RpS6 is an indicator that best reflects the healing process in the skin and the state of the vascular system [25]. We found that the stem cell group with the highest RpS6 immunoreactivity was also the best group in the burned skin samples taken on the 70th day after being burned. This result shows that the stem cell group, in which we observed the best results in terms of wound healing, was also the best healing group histologically.

Oxidative stress caused by burns is one of the links in a chain of events, in which dead cell particles in burned skin cause first local and then systemic damage [36]. It has been reported that postburn systemic oxidative stress, systemic inflammation, and end-organ damage occur on the 4th day [19]. Our findings suggest that early excision and removal of damaged skin from the body after burns may reduce resulting systemic oxidative stress. Furthermore, our results show that ADSC further reduces tissue damage and systemic oxidative stress by reducing local inflammation in the acute period of burn injury. This finding is suggestive of the effective immunomodulatory activity of ADSC [37].

In a study, it was reported that IL-6 was the first biomarker produced in systemic inflammation after burn trauma [38,39]. In our study, we found that the level of IL-6 was significantly lower in early excision treatments (stem cell group and early excision group) on the 4th day after the burn. IL-6 levels were lower in the PLM group than in the burn group, but higher than in the other groups.

Hydroxyproline and TGF-β1 levels can be used together to assess the healing of burned skin wounds [7,40]. In our study, the levels of hydroxyproline in the skin 96 h following the burn injury were found to be highest in the stem cell group. TGF-β levels were found to be highest in the stem cell group. Although hydroxyproline levels were higher in the burn group compared to the PLM and early excision groups, there was no significant difference in TGF-β levels. Based on these findings, we believe that wound healing in the burn area is more active in the stem cell group on the 4th day of healing.

The use of stem cell therapy in burn trauma is a relatively new and important area of research. A study on intradermal injection of ADSC has not been conducted for the treatment of severe burns covering 30% of TBSA in 3rd degree deep burns. Our study is one of the first one to address this mode of therapy and therefore, it is unique and novel. Kareem et al., the use of stem cell therapies in the topic of burn trauma and potential treatment mechanisms were described in detail [10]. They stated that the successful healing of a burn wound relies on the long-term presence of multiple growth factors, chemokines, and cytokines in a specific pattern [10].

Similarly, two other studies have suggested that the mechanism by which stem cell treatment potentially heals burn wounds is not through the proliferation of cells in the wound, but through regulation of chemokines, healing factors, and cytokine release in the affected area [41,42]. Our data showed that the regenerative capacity of ADSC also contributes to wound healing following burns. We speculate that stem cell therapy promotes angiogenesis, immunomodulation, and keratinocyte proliferation in wound healing, but it may also transform stem cells into newly healed skin tissue.

Ring et al. claimed that RpS6 could be used as a strong healing marker for burned skin, and that RpS6 elevation was an indication of good wound healing in skin tissue [25]. In our study, the best wound healing response was observed in the stem cell-treated group. The stem cell group also showed the highest level of RpS6 immunoreactivity in the skin.

Another important problem in burn wound healing is the development of scar formation in the wound. Various studies have reported that there is no scar formation after treatment with both bone marrow derived stem cells (BMSC) and adipose tissue-derived stem cells (ADSC) [43–47]. ADSCs can also regulate the release of chemokines, such as VEGF, and regulate the angiogenesis during wound healing [48].

In our study, on the 4th day the Nrf-2 level in the healed skin of the stem cell group was not different from the control group and was higher than the burn group and PLM group. We believe that high Nrf-2 levels are an important indicator for wound healing. Also, Nrf-2 levels are important indicators of antioxidant mechanisms. Oxidative stress caused by burns negatively affects wound healing. A high Nrf-2 level both reduces oxidative stress and creates a favorable environment for wound healing. If the Nrf-2 expression is abnormal hypertophic scar tissue formation may be observed [49]. ADSC may be effective against the formation of scar tissue and hypertrophic scars [49]. Our study lasted a total of 70 days, and at the end of this period, all of the rats in the stem cell group had closed burn wounds and had not developed hypertrophic scars.

This study has some limitations. First, it was an experimental study involving rats, and the results may not apply to humans. Second, there was no group for stem cell treatment (without excision) in the study of severe burns. Nevertheless, we tried to simulate the actual scenario in the burn clinics and our results are novel.

6. Conclusion

In this study, we evaluated the efficacy of intradermal stem cell injection and postburn early excision treatments on wound healing and oxidative stress following extensive and deep burns. The results of our study have shown to

important points. Early excision is an important treatment method to control both oxidative stress and the systemic inflammatory response in the early period after burn injury. ADSCs' may reduce the negative effects of inflammation on wounds by providing immunomodulation in the early phases of burns. Furthermore, ADSCs may modulate the microenvironment to promote scarless wound healing in large burn areas. We believe that early excision, along with intradermal injection of stem cells, may provide a new hope for patients with massive or severe third-degree deep burns that lack sufficient autograft options.

Ethical Approval

This experimental study was approved by the Animal Experiments Ethics Committee of İnönü University (Decision Number 2022/6–1).

Authorship

All authors meet all four authorship criteria as defined by the ICMJE guidelines.

Funding

This work was supported by İnönü University's Scientific Research Project Coordination Unit (project code TSA-2022–2989).

Declaration of Competing Interest

None

Acknowledgements

We would like to thank Suat Tekin, Engin Korkmaz, Asiye Beytur, and Onur Özkaya for their contributions to this study.

Appendix A. Supporting information

Supplementary data associated with this article can be found in the online version at doi:10.1016/j.burns.2024.07.037.

REFERENCES

[1] Wolf SE, Cancio LC, Pruitt BA. Epidemiological, demographic and outcome characteristics of burns. In: Herndon DN, editor. Total Burn Care. 5th ed.,Philadelphia: Elsevier; 2018. p. 14–27.
[2] ISBI Practice Guidelines Committee; Steering Subcommittee; Advisory Subcommittee. ISBI Practice Guidelines for Burn Care. Burns 2016;42:953–1021.
[3] Tejiram S, Romanowski KS, Palmieri TL. Initial management of severe burn injury. Curr Opin Crit Care 2019;25:647–52. https://doi.org/10.1097/MCC.0000000000000662
[4] Meuli JN, Pantet O, Berger MM, Waselle L, Raffoul W. Massive burns: retrospective analysis of changes in outcomes indicators across 18 years. J Burn Care Res 2022;43:232–9. https://doi.org/10.1093/jbcr/irab072
[5] Walker H, Chipp E. Short and long term mortality following massive burn injury (> 50% TBSA) in a UK burns centre. Burns 2022;48:1845–9. https://doi.org/10.1016/j.burns.2022.02.006
[6] Shokrgozar MA, Fattahi M, Bonakdar S, Ragerdi Kashani I, Majidi M, Haghighipour N, et al. Healing potential of mesenchymal stem cells cultured on a collagen-based scaffold for skin regeneration. Iran Biomed J 2012;16:68–76. https://doi.org/10.6091/ibj.1053.2012
[7] Abdel-Gawad DRI, Moselhy WA, Ahmed RR, Al-Muzafar HM, Amin KA, Amin MM, et al. Therapeutic effect of mesenchymal stem cells on histopathological, immunohistochemical, and molecular analysis in second-grade burn model. Stem Cell Res Ther 2021;12:308. https://doi.org/10.1186/s13287-021-02365-y
[8] Öksüz S, Ülkür E, Öncül O, Köse GT, Küçükodac Z, Urhan M. The effect of subcutaneous mesenchymal stem cell injection on statis zone and apoptosis in an experimental burn model. Plast Reconstr Surg 2013;131:463–71. https://doi.org/10.1097/PRS.0b013e31827c6d6f
[9] Yang Y, Zhang W, Li Y, Fang G, Zhang K. Scalded skin of rat treated by using fibrin glue combined with allogeneic bone marrow mesenchymal stem cells. Ann Dermatol 2014;26:289–95. https://doi.org/10.5021/ad.2014.26.3.289
[10] Abdul Kareem N, Aijaz A, Jeschke MG. Stem cell therapy for burns: story so far. Biologics 2021;15:379–97. https://doi.org/10.2147/BTT.S259124
[11] Hassan WU, Greiser U, Wang W. Role of adipose-derived stem cells in wound healing. Wound Repair Regen 2014;22:313–25. https://doi.org/10.1111/wrr.12173
[12] Rangatchew F, Vester-Glowinski P, Rasmussen BS, Haastrup E, Munthe-Fog L, Talman ML, et al. Mesenchymal stem cell therapy of acute thermal burns: a systematic review of the effect on inflammation and wound healing. Burns 2021;47:270–94. https://doi.org/10.1016/j.burns.2020.04.012
[13] Yamanaka S. Pluripotent stem cell-based cell therapy-promise and challenges. Cell Stem Cell 2020;27:523–31. https://doi.org/10.1016/j.stem.2020.09.014
[14] Zuk PA, Zhu M, Mizuno H, Huang J, Futrell JW, Katz AJ, et al. Multilineage cells from human adipose tissue: implications for cell-based therapies. Tissue Eng 2001;7:211–28. https://doi.org/10.1089/107632701300062859
[15] Mazini L, Rochette L, Amine M, Malka G. Regenerative capacity of adipose derived stem cells (ADSCs), comparison with mesenchymal stem cells (MSCs). Int J Mol Sci 2019;20:2523. https://doi.org/10.3390/ijms20102523
[16] Chu DT, Nguyen Thi Phuong T, Tien NLB, Tran DK, Minh LB, Thanh VV, et al. Adipose tissue stem cells for therapy: an update on the progress of isolation, culture, storage, and clinical application. J Clin Med 2019;8:917. https://doi.org/10.3390/jcm8070917
[17] Gürünlüoğlu K, Demircan M, Taşçı A, Üremiş MM, Türköz Y, Bağ HG, et al. The effects of two different burn dressings on serum oxidative stress indicators in children with partial burn. J Burn Care Res 2019;40:444–50. https://doi.org/10.1093/jbcr/irz037
[18] El Ayadi A, Herndon DN, Finnerty CC. Biomarkers in burn patient care. In: Herndon DN, editor. Total Burn Care. 5th ed.,Philadelphia: Elsevier; 2018. p. 232–5.
[19] Aslan M, Gül M, Üremiş N, Akbulut S, Gürünlüoğlu S, Özsoy EN, et al. 96th-hour impact of scalding burns on end organ damage, systemic oxidative stress, and wound healing in rats treated with three different types of dressings. J Burn Care Res 2024;45(3):733–43. https://doi.org/10.1093/jbcr/irad191
[20] Haller HL, Sander F, Popp D, Rapp M, Hartmann B, Demircan M, et al. Oxygen, pH, lactate, and metabolism-how old knowledge and new insights might be combined for new wound treatment. Medicina 2021;57:1190. https://doi.org/10.3390/medicina57111190
[21] Roshangar L, Soleimani Rad J, Kheirjou R, Reza Ranjkesh M, Ferdowsi Khosroshahi A. Skin burns: review of molecular

mechanisms and therapeutic approaches. Wounds 2019;31:308–15. PMID: 31730513.
[22] Sharda D, Ghosh S, Kaur P, Basu B, Choudhury D. Chitosan-insulin nano-formulations as critical modulators of inflammatory cytokines and Nrf-2 pathway to accelerate burn wound healing. Discov Nano 2023;18:154. https://doi.org/10.1186/s11671-023-03941-2
[23] Chang KC, Ma H, Liao WC, Lee CK, Lin CY, Chen CC. The optimal time for early burn wound excision to reduce pro-inflammatory cytokine production in a murine burn injury model. Burns 2010;36:1059–66. https://doi.org/10.1016/j.burns.2010.02.004
[24] Demircan M, Gürünlüoğlu K, Gözükara Bağ HG, Koçbıyık A, Gül M, Üremiş N, et al. Impaction of the polylactic membrane or hydrofiber with silver dressings on the interleukin-6, tumor necrosis factor-α, transforming growth factor-b3 levels in the blood and tissues of pediatric patients with burns. Ulus Travma Acids Cerrah– Derg 2021;27:122–31. https://doi.org/10.14744/tjtes.2020.30483
[25] Ring NAR, Dworak H, Bachmann B, Schädl B, Valdivieso K, Rozmaric T, et al. The p-rpS6-zone delineates wounding responses and the healing process. Dev Cell 2023;58:981–92. https://doi.org/10.1016/j.devcel.2023.04.001
[26] Eshar D, Huckins GL, Shrader TC, Beaufrère H. Comparison of intramuscular administration of alfaxalone-ketamine-dexmedetomidine and alfaxalone-butorphanol-midazolam in naked mole-rats (Heterocephalus glaber). Am J Vet Res 2019;80(12):1089–98. https://doi.org/10.2460/ajvr.80.12.1089
[27] Sowa Y, Imura T, Numajiri T, Nishino K, Fushiki S. Adipose-derived stem cells produce factors enhancing peripheral nerve regeneration: influence of age and anatomic site of origin. Stem Cells Dev 2012;21:1852–62. https://doi.org/10.1089/scd.2011.0403
[28] Zuk PA, Zhu M, Ashjian P, De Ugarte DA, Huang JI, Mizuno H, et al. Human adipose tissue is a source of multipotent stem cells. Mol Biol Cell 2002;13:4279–95. https://doi.org/10.1091/mbc.e02-02-0105
[29] Rahal OM, Nie L, Chan LC, Li CW, Hsu YH, Hsu J, Yu D, Hung MC. Selective expression of constitutively active pro-apoptotic protein BikDD gene in primary mammary tumors inhibits tumor growth and reduces tumor initiating cells. Am J Cancer Res 2015;5(12):3624–34.
[30] Sharma N, Arya G, Kumari RM, Gupta N, Nimesh S. Evaluation of anticancer activity of silver nanoparticles on the A549 human lung carcinoma cell lines through alamar blue assay. BioProtoc 2019;9:e3131https://doi.org/10.21769/BioProtoc.3131
[31] Chu YW, Wang R, Schmid I, Sakamoto KM. Analysis with flow cytometry of green fluorescent protein expression in leukemic cells. Cytometry 1999;36(4):333–9. https://doi.org/10.1002/(sici)1097-0320(19990801)36:4<333::aid-cyto8>3.0.co;2-f
[32] Gilpin DA. Calculation of a new Meeh constant and experimental determination of burn size. Burns 1996;22:607–11.
[33] Gouma E, Simos Y, Verginadis I, Lykoudis E, Evangelou A, Karkabounas S. A simple procedure for estimation of total body surface area and determination of a new value of Meeh's constant in rats. Lab Anim 2012;46:40–5.
[34] Livak KJ, Schmittgen TD. Analysis of relative gene expression data using real-time quantitative PCR and the 2– ΔΔCT method. METHODS 2001;25:402–8.
[35] Parihar A, Parihar MS, Milner S, Bhat S. Oxidative stress and anti-oxidative mobilization in burn injury. Burns 2008;34:6–17. https://doi.org/10.1016/j.burns.2007.04.009
[36] Ozcan O, Ipekci H, Alev B, Ustundag UV, Ak E, Sen A, et al. Protective effect of Myrtle (Myrtus communis) on burn induced skin injury. Burns 2019;45:1856–63. https://doi.org/10.1016/j.burns.2019.07.015
[37] Al-Ghadban S, Bunnell BA. Adipose tissue-derived stem cells: immunomodulatory effects and therapeutic potential. Physiol (Bethesda) 2020;35(2):125–33. https://doi.org/10.1152/physiol.00021.2019
[38] Agay D, Andriollo-Sanchez M, Claeyssen R, Claeyssen R, Touvard L, Denis J, et al. Interleukin-6, TNF-alpha and Interleukin-1 beta levels in blood and tissue in severely burned rats. Eur Cytokine Netw 2008;19:1–7. https://doi.org/10.1684/ecn.2008.0113
[39] Barayan D, Abdullahi A, Vinaik R, Knuth CM, Auger C, Jeschke MG. Interleukin-6 blockade, a potential adjunct therapy for post-burn hypermetabolism. FASEB J 2021;35:e21596https://doi.org/10.1096/fj.202100388R
[40] Karakaya E, Akdur A, Ayvazoğlu Soy E, Araz C, Ok Atilgan A, Özturan Özer E, et al. Effect of subcutaneous topical ozone therapy on second-degree burn wounds in rats: an experimental study. J Burn Care Res 2021;42:1243–53. https://doi.org/10.1093/jbcr/irab110
[41] Ghieh F, Jurjus R, Ibrahim A, Geagea AG, Daouk H, El Baba B, et al. The use of stem cells in burn wound healing: a review. Biomed Res Int 2015;2015:684084https://doi.org/10.1155/2015/684084
[42] Nourian Dehkordi A, Mirahmadi Babaheydari F, Chehelgerdi M, Raeisi Dehkordi S. Skin tissue engineering: wound healing based on stem-cell-based therapeutic strategies. Stem Cell Res Ther 2019;10:111. https://doi.org/10.1186/s13287-019-1212-2
[43] Liu J, Ren J, Su L, Cheng S, Zhou J, Ye X, Dong Y, et al. Human adipose tissue-derived stem cells inhibit the activity of keloid fibroblasts and fibrosis in a keloid model by paracrine signaling. Burns 2018;44:370–85. https://doi.org/10.1016/j.burns.2017.08.017
[44] Fang F, Huang RL, Zheng Y, Liu M, Huo R. Bone marrow derived mesenchymal stem cells inhibit the proliferative and profibrotic phenotype of hypertrophic scar fibroblasts and keloid fibroblasts through paracrine signaling. J Dermatol Sci 2016;83:95–105. https://doi.org/10.1016/j.jdermsci.2016.03.003
[45] Trottier V, Marceau-Fortier G, Germain L, Vincent C, Fradette J. IFATS collection: using human adipose-derived stem/stromal cells for the production of new skin substitutes. Stem Cells 2008;26:2713–23. https://doi.org/10.1634/stemcells.2008-0031
[46] Maharlooei MK, Bagheri M, Solhjou Z, Jahromi BM, Akrami M, Rohani L, et al. Adipose tissue derived mesenchymal stem cell (AD-MSC) promotes skin wound healing in diabetic rats. Diabetes Res Clin Pr 2011;93:228–34. https://doi.org/10.1016/j.diabres.2011.04.018
[47] Alexaki VI, Simantiraki D, Panayiotopoulou M, Rasouli O, Venihaki M, Castana O, et al. Adipose tissue-derived mesenchymal cells support skin reepithelialization through secretion of KGF-1 and PDGF-BB: comparison with dermal fibroblasts. Cell Transpl 2012;21:2441–54. https://doi.org/10.3727/096368912x637064
[48] Kode JA, Mukherjee S, Joglekar MV, Hardikar AA. Mesenchymal stem cells: immunobiology and role in immunomodulation and tissue regeneration. Cytotherapy 2009;11:377–91. https://doi.org/10.1080/14653240903080367
[49] Li S, Yang J, Sun J, Chen M. Adipose-derived mesenchymal stem cells alleviate hypertrophic scar by inhibiting bioactivity and inducing apoptosis in hypertrophic scar fibroblasts. Cells 2022;11:4024. https://doi.org/10.3390/cells11244024